Evolutionary drivers of morphological differentiation among three bottlenose dolphin lineages, *Tursiops* spp. (Delphinidae), in the northwest Indian Ocean utilising linear and geometric morphometric techniques

Howard Gray[1], Koen Van Waerebeek[2], Joseph Owen[3], Tim Collins[4], Gianna Minton[5], Louisa Ponnampalam[6], Andrew Willson[7], Robert Baldwin[8] & A. Rus Hoelzel[1*]

1) Department of Biosciences, University of Durham, South Road, Durham DH1 3LE, UK
2) Centro Peruano de Estudios Cetológicos, Lima-20, Peru & CMMRL, Santiago de Chile
3) Department of Archaeology, Simon Fraser University, Education Building 9635, 8888 University Dr Burnaby, Burnaby, British Columbia, Canada V5A 1S6
4) Wildlife Conservation Society Ocean Giants Program, 2300 Southern Blvd, Bronx, NY 10460-1099, USA.
5) Megaptera Marine Conservation, Den Haag, The Netherlands.
6) The MareCet Research Organization, 40460 Shah Alam, Malaysia
7) Future Seas Global SPC, PO Box 286, Postal Code 116, Muscat, Sultanate of Oman.
8) Five Oceans Environmental Services, PO Box 660, PC131, Ruwi, Sultanate of Oman.
*Correspondence

Running title:

Bottlenose dolphin morphological differentiation

Abstract

Local adaptation and adaptive radiations are typically associated with phenotypic variation suited to alternative environments. In the marine environment, the nature of relevant ecological or environmental transitions is poorly understood, especially for highly mobile species. Here we compare three genetic lineages in the genus *Tursiops* (bottlenose dolphins), using linear measurements and geometric morphometric techniques, in the context of environmental variation in the northwest Indian Ocean. Cranial morphology was clearly differentiated comparing *T. truncatus* and *T. aduncus*, while a recently discovered genetic lineage, found in the Arabian Sea, was morphologically most similar to *T. aduncus* from the same region, but distinct for various measures, particularly metrics associated with the lateral dimension of the skull. The extent of divergence between *T. truncatus* and *T. aduncus* compared to differences between the *T. aduncus* lineages is consistent with the recent phylogeny for these species. Therefore, with the corroboration of genetic and morphological inference, we propose two conservation units of *T. aduncus* be recognised in the region at a sub-specific level so that their conservation can be managed effectively. We consider possible evolutionary mechanisms associated with regional habitat characteristics and the exploitation of distinct prey resources.

Keywords
adaptation, Indian Ocean, divergence, morphology, speciation

Introduction

It has become common for questions of taxonomic classification to focus on inference from molecular genetic phylogenies, though significant challenges remain (e.g. associated with assessing phylogenetic uncertainty; see Yang & Rannala, 2012). The phylogenetic approach has been especially important for groups of organisms where there is substantial variation in morphology, but difficulties exist with identifying consistent morphological synapomorphies (e.g. Dalebout *et al*. 2008, Dornburg *et al*. 2015). At the same time, in the context of molecular data, patterns of phenotypic variation are important in support of determining the distinction between regional variation and alpha taxonomy (e.g. Moura *et al*. 2020). Phenotypic variation is directly exposed to selection and can therefore reveal the evolutionary drivers and mechanisms supporting species radiation. In this study we focus on the genus *Tursiops*, which has historically been proposed to include up to 20 species, based on morphometric characters (though sometimes based on quite limited data; Hershkovitz,

1966), and as few as just one (*T. truncatus*). In particular, we investigate the morphological characteristics of a genetically distinct lineage of bottlenose dolphin most closely related to the Australasian lineage of *T. aduncus* that has been recently identified off India, Pakistan and Oman (Gray *et al*. 2018, Moura *et al*. 2020).

In a worldwide comparison of *Tursiops* populations, based on mtDNA control region sequences and microsatellite markers, Natoli *et al*. (2004) found considerable genetic diversity and differentiation among all populations studied. Results supported the designation of *T. aduncus* (Ehrenberg, 1833), as put forward by Wang *et al*. (1999), as a species distinct from *T. truncatus* (Montagu, 1821). Further results revealed the presence of another distinct lineage of *T. aduncus* from South Africa. This inference was later supported in phylogenies based on whole mitogenomes (Moura *et al*. 2013) and 4MB from the nuclear genome (Moura *et al*. 2020). Moura *et al*. (2020) found support from their nuclear phylogenomic study for a monophyletic *Tursiops* genus divided into two main lineages representing the species *T. aduncus* and *T. truncatus*. Each species was further divided into regional lineages, including that representing the Indian Ocean (IO) *T. aduncus* type.

The *T. aduncus* holotype was originally described from an individual stranded on an island in the Dahlak Archipelago in the Red Sea. A sequence of the mtDNA control region from this specimen revealed it to be related to populations off South Africa (Perrin *et al*. 2007). Mitogenomic phylogenies of *T. aduncus* in the western IO support the presence of a new *T. aduncus* lineage in the Arabian Sea, off India, Pakistan and Oman (which was monophyletic and differentiated from the Australasian and South African lineages; Gray *et al*. 2018). The range of the *T. aduncus* holotype mtDNA lineage extends into this region (the dominant lineage amongst Oman samples, and rare amongst those from India and Pakistan) suggesting these lineages are coming into secondary contact (Gray *et al*. 2018). In India, Jayasankar *et al*. (2008) identified bottlenose dolphin individuals to be *T. aduncus* based on partial mtDNA cytochrome-*b* sequences. One haplotype was shared with a Japanese individual sequenced by Shirakihara *et al*. (2003), suggesting the Indian peninsula might also be a transitional occurrence zone for the Chinese/Australasian *T. aduncus* (Wang *et al*. 1999).

Concordance between morphology and the phylogenetic relationships reported in Gray *et al*. (2018) would strengthen support (see Reeves *et al*. 2004) for the proposed novel *T. aduncus* lineage and facilitate inference about the evolutionary processes generating differentiation. If the drivers are environmental, other regional species may show similar parallel patterns of differentiation. Several other studies and reviews have incorporated the use of morphometric data from small cetacean skeletal remains from the region, predominantly Oman. Cetaceans examined have included humpback dolphins, *Sousa* spp.

(Baldwin *et al*. 2004; Jefferson & Van Waerebeek, 2004) spinner dolphins, *Stenella longirostris*, rough toothed dolphins, *Steno bredanensis*, melon-headed whales, *Peponocephala electra* (Van Waerebeek *et al.* 1999) and common dolphins, *Delphinus* spp. (Jefferson & Van Waerebeek, 2002). Gray *et al*. (2018) discussed a possible context for differentiation on either side of the Sea of Oman associated with climate change during the early Holocene, suggesting that changes to the southwest monsoons altered distributions of habitat and available prey, possibly through an increase in turbidity in nearshore waters, generating an ecological barrier.

As the human populations expand and coastlines in the northwest IO are developed, fisheries activities, areas of construction, shipping and oil exploration overlap increasingly with identified habitat for many small cetacean species and pose a threat to regional populations (IWC, 1999; Collins *et al.* 2002; Baldwin *et al*. 2004; Minton *et al*. 2010, Anderson, 2014).

Here, we utilise linear and geometric morphometric techniques to explore the morphological relationships between three putative bottlenose dolphin evolutionary significant units in the region: (i) *T. aduncus* holotype lineage, (ii) *T. aduncus*, Arabian Sea lineage and (iii) *T. truncatus*. Such information will be important for taxonomic level classification, and effective conservation and management of coastal cetaceans in the region (Mace, 2004; Reeves *et al*. 2004). More broadly, local morphological adaptation in highly mobile marine taxa currently experiencing secondary contact (or sympatric speciation) in the northwest IO will provide insight into evolutionary processes, and associated environmental drivers, operating in the region.

Materials and Methods

Bottlenose dolphin (*Tursiops* spp.) specimens, collected along Oman's coast, were curated at the Oman Natural History Museum (ONHM; n = 80) and specimens collected in Pakistan (n = 10) and Iran (n = 1) were curated at the Museum am Löwentor, Staatliches Museum für Naturkunde, in Stuttgart, Germany (SMNS). All of the ONHM specimens were beach-cast individuals, the skeletal remains of which were collected on various survey expeditions across Oman, predominantly led by independent scientists, the Oman Whale and Dolphin Research Group, Five Oceans Environmental Services (5OES) and the Environment Society of Oman (ESO). Specimens curated at the SMNS were collected in Pakistan around the Indus River Delta and the Strait of Hormuz (Iran) on expeditions by G. Pilleri and M. Gihr (1971-9; Figure 1).

Where DNA extraction was successful (n = 73), specimens were assigned to a *Tursiops* lineage based on their placement within a phylogeny generated using mtDNA control region sequences (404 bp) (Figure S1). Within this phylogeny we include Australasian *T. aduncus* sequences from GenBank (Wang *et al*. 1999), however none of our samples fell within this fourth lineage. The lineages for our samples were: (i) holotype *T. aduncus* (Hol-Ta; Perrin et al. 2007), (ii) Arabian Sea *T. aduncus* (AS-Ta; Gray *et al*. 2018, Gray *et al*. 2021), and (iii) *T. truncatus* (Tt). Lineage assignment of sequences was supported by an unsupervised clustering analysis (Rodriguez & Laio, 2014) in R using the *densityClust* package (Pedersen *et al*. 2016) (Figure S2). Specimens that could not be assigned to a genetic lineage, due to unsuccessful DNA extraction, were omitted from analyses where *a priori* group information was required e.g. LDA (see below). However, lineage assignments were predicted based on morphology, using cluster analysis and models generated from morphological data where specimen assignment to a lineage was known (see below). To eliminate variability associated with developmental growth, only specimens considered cranially adult (or sub-adult), based on fusion of maxillary plates to the cranium (Ross & Cockcroft, 1990; Kemper, 2004), were included in morphometric analyses.

Measurements of 40 cranial characters were taken (Figure 2 and Table S1). Measurements up to 150 mm were taken to the nearest 0.02 mm, measurements between 150 mm - 300 mm were taken to the nearest 0.05 mm and all measurements greater than 300 mm were taken to the nearest millimetre. Specimens were assigned single upper (TTU) and lower (TTL) tooth counts using the highest counts among the two sides (Amaha, 1994; Jefferson & Van Waerebeek, 2002).

Measurements were not attempted where characters were damaged, thus resulting in missing data. To investigate intra-observer error, all measurements were taken in triplicate. Repeat measurements were taken ‘blindly’, i.e., without prior knowledge of previous measurements taken. It was assumed that cranial characters measured with a percentage error of > 1% across repeats were measured unreliably, and therefore omitted from analyses. The sex of a specimen was not typically known, however various earlier studies found little or no sexual dimorphism for cranial measurements in *Tursiops* spp. (Hersh *et al*. 1990, Kemper 2004, Ross 1977). Moreover, there was no reason to suspect a significantly biased gender composition.

Because multivariate analyses are sensitive to missing data (Kim & Curry, 1977), characters missing measurements for more than 20% of the cranially mature specimens were removed from analyses (18 characters retained, see Results). Any specimens with more than 30% missing data for the remaining characters were also removed (see Results). This was

done to minimise the number of specimens with missing data, thereby limiting error introduced through value substitution (Brown *et al*. 2012), while maximising statistical power. The mean value of available data for a character was substituted for remaining missing data (e.g. Jefferson & Van Waerebeek, 2002).

All statistical analyses performed on the linear measurements were conducted in R (R Core Team, 2013). A *k*-medoids cluster analysis was performed using *cluster* (Maechler *et al*. 2015). Under this method, a cluster is represented by a data point (medoid) rather than the mean of its constituents (as in the *k*-means algorithm), thus making it more robust to outliers and 'noisy' data. Silhouette clustering was carried out to determine the optimal number of clusters. This method considers how close data points are to neighbouring clusters. Silhouette values for each data point (specimen) provide an indication of how well the clusters are separated (Kaufman & Rousseeuw, 2009). The highest average silhouette width for different values of *k* is indicative of the most optimal number of clusters to consider. The function *clusplot* was used to plot ellipses around respective clusters on a Principal Component Analysis (PCA).

A linear discriminant analysis (LDA) was carried out using the *lda* function in the R *MASS* package (Venables & Ripley, 2002). This analysis included only individuals that were sequenced and genetically assigned to a lineage (Hol-Ta, AS-Ta or Tt) *a priori*. A MANOVA was carried out using the *stats* package (R Core Team, 2013) to test whether character measurements were statistically significant between groups. A stepwise selection of characters was carried out using the *greedy.wilks* function in the *klaR* package (Weihs *et al*. 2005) to ascertain which characters were the most important for discriminating between groups. The Wilks' lambda criterion is used to retain characters with relatively high importance and omit those with low explanatory power. The procedure begins with the character that explains the most separation between groups. New characters are then added in a stepwise fashion by selecting those that minimise the Wilks' lambda of the model, including it if the *P*-value still shows statistical significance (using a *niveau* = 0.1 threshold). Leave-one-out cross-validation analysis was performed on the characters most important for discriminating between groups. A further MANOVA was performed on the *T. aduncus* specimens to assess whether character dimensions differed significantly between the two lineages (Hol-Ta and AS-Ta).

Various checks were performed to assess whether the data met assumptions required for parametric tests, which included, among others, tests for multivariate normality, homogeneity of variances and homogeneity of variance-covariance matrices. Such assumptions are frequently violated in morphometric datasets, especially when sample sizes

are low (Bocxlaer & Schultheiß, 2010). Therefore, a non-parametric multivariate Kruskal-Wallis test was performed using the *multkw* function in the *ULT* package (He *et al*. 2017). In addition, a Random Forest (RF) classification algorithm, which makes no underlying assumptions about the data, was implemented using the *randomForest* package (Liaw & Wiener, 2002). After tuning, the *mtry* parameter was set to 18 and *ntrees* to 1500. The proximity matrix from the model was plotted as a PCA using the *MDSplot* function to visualise the cluster assignments as a 2D projection.

A total of 52 cranially mature (see above) and intact *Tursiops* spp. skulls from ONHM and eight skulls from SMNS were photographed for geometric morphometric (GM) analysis. 39 Landmarks (LMs; Figure 3, Table S2) were digitised on the left side of the skull for each aspect (dorsal, ventral and lateral) using TpsDig 2.05 (Rohlf, 2005).

In order to control for error introduced by specimen orientation during photography and LM digitisation, a series of tests and checks were carried out. LMs were digitised 'blindly' three times on a single photo for a subset of specimens (n = 13). A PCA was performed in MORPHOJ v. 1.05f (Klingenberg, 2011) following a Generalised Procrustes Analysis (GPA), performed in MORPHEUS ET AL. (Slice, 1998). Tight clustering of repeats suggests error in landmark digitisation was minimal compared to inter-specimen variation. Euclidean distances of LMs to configuration centroids were used to calculate percentage errors across repeats for each specimen (Singleton, 2002). All LMs that showed <1% error were included in further tests. LMs that showed good repeatability were digitised for each specimen's photo triplicate. A GPA was conducted on all triplicates for all specimens in MORPHEUS ET AL. Procrustes-fit coordinates were used to calculate percentage error for each LM between pairs of photos within each triplicate, using Euclidean distances of LMs to centroids (as repeatability test). Configurations that showed the least error across LMs in this comparison were retained for further analyses (i.e. omitting data from the third photo). This was done to minimise orientation error introduced during photography. Where intra-specimen LM digitisation error was high (> 1.5%), LMs were omitted and treated as missing data. Where inter-specimen LM digitisation error was high across all specimens (> 1.5%), LMs were omitted from analyses. Specimens missing more than four LMs were also omitted from analyses.

Coordinates for missing LMs were estimated using the thin-plate spline method implemented using the *estimate.missing* function in the R package *geomorph* (Adams & Otarola-Castillo, 2013). The Procrustes group average for all available data was used as the reference configuration for estimating missing LMs in target configurations (Mitteroecker & Gunz, 2009). Once data were truncated (see Results) and missing LMs estimated, analyses

were conducted on Procrustes averaged configurations for each photo duplicate so that each specimen was represented by one configuration of LMs in each aspect.

Data were first submitted to a GPA in MORPHOJ v. 1.05f and a co-variance matrix was generated from the Procrustes-fit coordinates to enable PCA exploratory analysis of shape relationships between the specimens. A MANOVA was performed in R to test whether the PCs showed significant differences between genetically allocated groups. To visualise and compare average group shapes, thin-plate spline transformation grids and wireframe graphs were generated in MORPHOJ v. 1.05f (Klingenberg, 2011).

Size is represented by centroid size, which is the square root of the summed squared distances from the configuration centroid to each LM. To investigate the effects of allometry on the shape differences within groups, a pooled, within-group, multivariate regression analysis was performed on log centroid size (as the independent variable) and the Procrustes coordinates (as the multidimensional dependent variables of shape) in MORPHOJ v. 1.05f. A permutation test was performed (10,000 rounds) to investigate whether shape was significantly independent of size. To correct for the effects of allometry, a PCA was performed on the regression residuals and a MANOVA on the retained PCs (those which explained up to 80% of the total variance) was used to test for group differences in allometry-corrected shape. An ANOVA and Procrustes-ANOVA were performed in MORPHOJ v. 1.05f to test for differences between groups in size and shape, respectively.

A canonical variates analysis (CVA) and a discriminant function analysis (DFA), with leave-one-out cross-validation, was carried out on groups to which specimens were assigned *a priori* (see Results). For both the CVA and DFA analyses, differences in shape between groups were quantified as Mahalanobis distances, which is a measure of group differences relative to the variation within groups, and Procrustes distances, which is a measure of group deviation from the population average (Klingenberg & Monteiro, 2005). Associated *P*-values for each distance were generated from permutation tests (1000 rounds). All analyses were performed for each aspect and implemented in MORPHOJ v. 1.05f.

Results

After data truncation, the linear morphometrics dataset (SMNS $n = 8$, ONHM $n = 46$) included 18 characters across 54 individuals (Hol-Ta: $n = 29$, AS-Ta: $n = 9$, Tt: $n = 8$, unknown: $n = 8$). Measurements of characters used in analyses (for genetically assigned specimens) are summarised in Figure 4, while all measurements are detailed in Table S3. In the PCA, four PCs were identified based on a screeplot and accounted for 80.59% of the total variance, with PCs 1-4 explaining 41.17%, 20.17%, 10.71% and 8.53%, respectively. PC

loadings are given in Table S4. Two clusters were identified under the *k*-medoids algorithm, represented by known *T. aduncus*-type and *T. truncatus* specimens, with strong separation along PC1 (Figure 5). No specimens were incorrectly assigned to these clusters, supporting classification of specimens of unknown lineage as either *T. truncatus* or *T. aduncus* based on their assignments.

The LDA scatterplot of canonical scores separates the groups (Hol-Ta, AS-Ta and Tt) into three clusters (Figure 6). LD1 discriminated well between *T. truncatus* and *T. aduncus*-types, whereas LD2 separated Hol-Ta and AS-Ta, with some overlap. The characters contributing the most to separation along LD1 were measurements associated with the maxilla/premaxilla and lacrimal (RW60, RWM, RL, GWEN, UTLTR, LAL) as well as the temporal fossae (GLPTF, LWPTF). Characters contributing the most to separation along LD2 were measurements associated with skull widths (ZW and GPOW), rostral widths (RW75%, PRW), width of external nares (GWEN) and length of orbit (LO). The coefficients of linear discriminants are listed in Table S5. The percentages of separation achieved by LD1 and LD2 were 91.25% and 8.75%, respectively. Fourteen of the 18 measured characters differed significantly between groups (Wilks' lambda = 0.02, $F_{36, 52} = 8.00$ $P < 0.001$; see Table S3). A 'greedy' LDA was performed on five characters (RWM, RW60, LAL, GPOW & ZW) that were retained in a stepwise MANOVA and produced similar results. 'Mid-' rostral widths (RWM & RW60) and lacrimal bone (LAL) dimensions discriminated most between *T. truncatus* and *T. aduncus* along LD1, whereas the two skull widths (GPOW & ZW) contributed most to discriminating between the *T. aduncus* types along LD2. Differences between the *T. aduncus* lineages on the characters were deemed significant (Wilks' lambda = 0.29, $F_{18,19} = 2.53$, $P < 0.05$). Hol-Ta was larger in all measurements, but there was overlap for all characters examined (see Figure 4). Leave-one-out cross validation results revealed a 56% misclassification rate for AS-Ta individuals and 17% for Hol-Ta individuals. Misclassification rates within the *T. aduncus*-type lineages suggest that the morphologies of Hol-Ta and AS-Ta overlap. Most Tt individuals were correctly assigned with a 13% misclassification rate (Table 2). Overall, the misclassification rate was 24%, but sample sizes for AS-Ta and Tt groups were low.

A number of assumptions for multivariate parametric testing were not met by the linear measurement dataset. One underlying problem was that the within-group (lineage) sample sizes were low for two of the three lineages. Within-lineage box-whisker plots revealed a number of univariate outliers (Figure S3) and within-lineage multivariate normality was absent for a number of characters (Hol-Ta: GPOW, RW60, LAL; AS-Ta: GWEN, GPRW, GWIN; Tt: RWM) based on the Shapiro-Wilk test ($P < 0.05$). Exploration

of correlation matrices and Variance Inflation Factors suggested multicollinearity was present. Moreover, Box's M test of equality of covariance was highly significant ($M = 792$, $p < 0.001$), suggesting an absence of homogeneity, and Levene's test of homogeneity of variance was significant ($P < 0.05$) for GWPX, GPRW, GWIN and LO, suggesting this was also absent. As a number of assumptions to these tests were violated, a non-parametric multivariate Kruskal-Wallis test was also performed, which confirmed that the morphological characters differed significantly between the lineages, $\chi^2(36) = 55.82$, $p = 0.019$. Kruskal Wallis tests for each character and post-hoc pairwise comparisons using Dunn's (1964) procedure, with Bonferroni correction, revealed differences between characters were limited to the inter-species level (*T. trunactus* vs *T. aduncus*) (Table S6).

The RF classification method, which does not rely on parametric assumptions, was able to distinguish between *T. aduncus* and *T. truncatus* without error. Misclassification between *T. aduncus* was more difficult, with 44% of AS-Ta misclassified as Hol-Ta, but only 7% of Hol-Ta misclassified as AS-Ta (Table 2, Figure 7). Characters identified as important for the model (Figure 8) were similar to those identified in the LDA with the exception of the greatest preorbital width (GPRW) which had both the highest 'mean decrease accuracy' and 'mean decrease Gini' in the random forest model but was deemed unimportant in the stepwise MANOVA. However, greatest post-orbital width (GPOW), a correlated measure ($r(44) = 0.86$, $p < 0.001$), was an important contributor to the LDA model in distinguishing between *T. aduncus*. Lineage classification predictions were the same under the *k*-medoids, LDA and random forest models specimens that remained genetically unassigned ($n = 8$).

After data truncation and estimation of missing LMs, the datasets used in the geometric morphometric analyses were as follows: (i) 10 LMs in dorsal aspect (Hol-Ta: $n = 32$, AS-Ta: $n = 10$, Tt: $n = 9$, unknown: $n = 8$), (ii) 13 LMs in ventral aspect (Hol-Ta: $n = 33$, AS-Ta: $n = 10$, Tt: $n = 9$, unknown: $n = 8$), and (iii) 14 LMs in lateral aspect (Hol-Ta: $n = 33$, AS-Ta: $n = 10$, Tt: $n = 9$, unknown: $n = 8$; Table S2). Morphological relationships of geometric data were explored using PCA in dorsal, ventral and lateral aspect. In dorsal aspect, PCs 1-5 accounted for 81.00% of the total variance (explaining 31.49%, 20.80%, 14.26%, 9.07% and 5.37%, respectively). In ventral aspect, PCs 1-7 accounted for a combined 83.06% of the total variance (25.25%, 23.08%, 10.98%, 7.85%, 6.63%, 6.61% and 3.71%, respectively). For the lateral aspect, PCs 1-8 accounted for 81.88% of the total variation (20.63%, 15.18%, 14.84%, 9.00%, 6.82%, 6.81%, 5.39% and 3.95%, respectively). PC coefficients are listed for each aspect in Tables S7-S9. Scatterplots of the first two principal components were plotted for each aspect and accounted for a combined 52.29%, 48.33% and 35.81% of the total variation in dorsal, ventral and lateral aspect, respectively.

For the dorsal aspect (Figure 9A), separation between *T. truncatus* and *T. aduncus* specimens was achieved at the extremes of PC1. The same holds true for PC2 in ventral aspect (Figure 9B) and PC1 in lateral aspect (Figure 9C). Separation between *T. aduncus* lineages was less pronounced, with almost no separation in dorsal and ventral aspect on PC1 and PC2 respectively, but good separation in the lateral aspect. MANOVAs on retained PCs for each aspect revealed significant shape differences between genetically assigned groups for all aspects (dorsal: Wilks' lambda = 0.40, $F_{10,88} = 5.49$, $P < 0.001$; ventral: Wilks' lambda = 0.18, $F_{14, 86} = 8.49$, $P < 0.001$; lateral: Wilks' lambda MANOVA = 0.21, $F_{16, 84} = 6.15$, $P < 0.001$). Retained PCs for all aspects were checked for MANOVA assumption violations. Within-lineage box-whisker plots for each aspect revealed potential univariate outliers on a number of PCs (Figures S4-S6). Shapiro Wilk's tests revealed multivariate normality within lineages was present for all PCs in dorsal and ventral aspect but not in lateral aspect, being absent in PC3 for Hol-Ta ($W = 0.88$, $p = 0.002$) and Tt ($W = 0.88$, $p = 0.03$) lineages. There was no evidence of multicollinearity between any PCs based on VIFs and inspection of corelation matrices. There was homogeneity of covariance matrices and variance for PCs based on Box's M tests and Levene's test ($P = 0.05$) in dorsal ($M = 38.2$, $p = 0.145$) and ventral ($M = 46.3$, $p = 0.82$) aspect. In lateral aspect, PCs violated this assumption ($M = 158$, $p = <0.001$) and homogeneity of variance was absent for PCs 4-5 ($P < 0.05$).

Thin-plate spline transformation grids illustrating shape differences from the total average configuration, with superimposed wireframe graphs, were generated for the average shapes of each genetic lineage in dorsal, ventral and lateral aspect (Figure 10). Comparisons between *T. aduncus* and *T. truncatus* showed pronounced shape differences in all aspects. Overall, differences in the relative positioning of LMs associated with the temporal crest suggest a wider cranium in *T. truncatus* compared to *T. aduncus* groups, but also suggest differences in temporal fossae shape. Other shape differences suggest *T. truncatus* has a shorter, stockier rostrum, as well as larger external nares and pterygoids. Shape differences between the *T. aduncus* groups were few in dorsal and ventral aspect but for a slightly more elongated or slender shape for AS-Ta, or differences in the positioning of the temporal crest. This was also true in lateral aspect, but the relative positioning of LMs around the orbit and temporal fossa (more anterior in AS-Ta) suggest AS-Ta has a narrower or tighter curvature to the orbit and/or anterior shape differences in the temporal fossa.

Size predicted 11.26%, 4.18% and 2.98% of the variance in shape for dorsal, ventral and lateral aspect, respectively. Permutation tests showed that shape was significantly dependent on size in dorsal ($P < 0.001$) and ventral ($P = 0.032$) aspect but not in lateral aspect ($P > 0.05$). Size corrected shape differences between groups remained significant in all

aspects (Wilks' lambda MANOVA for: dorsal = 0.24, $F_{10, 88} = 9.25$, ventral = 0.25, $F_{14,86} = 6.2478$, lateral = 0.25, $F_{14,86} = 6.2478$; $P < 0.001$ for all).

Analysis of Variance (ANOVA) and Procrustes ANOVA were performed to explore the group-wise differences in size and shape, respectively. A significant difference was detected between groups in size and shape for dorsal (size: $F_{2, 48} = 30.18$, $P < 0.001$, shape: $F_{32,768} = 4.27$, $P < 0.001$, Pillai's trace = 1.03, $P = 0.0027$), ventral (size: $F_{2, 49} = 61.38$, $P < 0.001$, shape: $F_{44, 1078} = 6.67$, $P < 0.001$, Pillai's trace = 1.34, $P < 0.001$) and lateral (size: $F_{2, 49} = 60.62$, $P < 0.001$, shape: $F_{48, 1176} = 5.48$, $P < 0.001$, Pillai's trace = 1.42, $P = 0.001$) aspects. When considering only *T. aduncus* groups, no significant differences were observed between groups for size in dorsal ($F_{1, 40} = 0.31$, $P = 0.58$), ventral ($F_{1, 41} = 0.01$, $P = 0.92$) or lateral ($F_{1, 41} = 0.65$, $P = 0.424$) aspects. Shape differences were not significant in dorsal aspect ($F_{16, 640} = 1.37$, $P = 0.15$, Pillai's trace = 0.35, $P = 0.63$). In ventral aspect, shape differences between *T. aduncus* groups were significant, although Pillai's trace statistic was not ($F_{22, 902} = 1.74$, $P = 0.02$, Pillai's trace = 0.57, $P = 0.34$). In contrast, a significant difference in lateral shape was observed between *T. aduncus* groups ($F_{24, 984} = 3.28$, $P < 0.001$, Pillai's trace = 0.77, $P < 0.05$).

CVA revealed a separation of *T. truncatus* specimens from *T. aduncus* specimens along CV1 for all aspects (dorsal, ventral and lateral). Along CV2 there was an indication of separation between the *T. aduncus* groups, with the separation being most prominent in lateral aspect (Figure 11). Mahalanobis and Procrustes distances between pairs of groups and associated *P*-values are presented in Table 3. Results suggest shape differences between *T. truncatus* and *T. aduncus* specimens are highly significant in all aspects. The shape differences between the *T. aduncus* groups are less pronounced, but significant, for all aspects when considering Mahalanobis distances between groups but not for Procrustes distances in dorsal or ventral.

Results of the pairwise DFAs are displayed in Table 4. DFAs between *T. aduncus* and *T. truncatus* correctly assigned specimens to groups for all aspects. Results between *T. aduncus* groups also showed good discrimination. The reliability of the discrimination between groups was tested using leave-one-out cross-validation, the results of which are in Table 5. The best discrimination in shape was between Hol-Ta and Tt with high percentages of specimens being correctly assigned to their respective groups (> 75%). There was poor discrimination between AS-Ta and Tt individuals for all aspects but sample sizes were smaller for this comparison (AS-Ta, $n = 10$; Tt, $n = 9$). Discrimination between Hol-Ta and AS-Ta was poor in dorsal and ventral aspect but was prominent in lateral aspect.

Discussion

Analyses of linear measurements and of geometric morphometric data generally yielded similar results. Both methodologies detected morphological differences between *T. truncatus* and *T. aduncus* and were also able to identify morphological differences between the *T. aduncus* lineages using discriminatory analyses (LDA and CVA/DFA).

Species-level morphological differences (between *T. truncatus* and *T. aduncus*)

Morphological differences between *T. truncatus* and *T. aduncus* have been reported elsewhere. Kemper (2004) noted differences in the shape and size of the temporal fossa between *T. truncatus* and *T. aduncus* off South Australia and found LWPTF (width between posterior borders of temporal fossae) to be an important character for distinguishing between the two species. Ross & Cockcroft (1990) also found LWPTF and MAJDTF (major diameter of anterior temporal fossa) to be important characters in PCA analysis. Charlton-Robb *et al*. (2011) did not find measurements associated with the temporal fossa to be important, although *T. aduncus* was under-represented in their morphological study, and so important characters may have been biased towards differences between *T. australis* and *T. truncatus*. Cranial variation of *T. truncatus* ecotypes in Californian waters showed that inshore forms have larger temporal fossae than offshore forms (Perrin *et al*. 2011). This suggests a link to different feeding ecologies, because the temporal fossa is the location for jaw muscle attachment (Mead & Fordyce, 2009).

Kemper (2004) noted from photos of *T. truncatus* and *T. aduncus* specimens in Wang *et al*. (2000), that the temporal fossae are smaller and more elliptical in *T. truncatus* and larger and more circular in *T. aduncus*, which may suggest a parallel difference in feeding ecology where the more consistently nearshore form (*T. aduncus*) has more developed temporal fossae. Consistently, we also find measurements associated with the temporal fossa (e.g. LWPTF & GLPTF; see Results) to be important characters for discriminating between *T. truncatus* and *T. aduncus*. Investigations into stomach contents of dolphins in the waters of Oman reveal bottlenose dolphins to be feeding in either inshore/coastal habitats or offshore (Ponnampalam *et al*. 2012). Although not identified to species in the paper, those feeding nearshore were from the Gulf of Masirah, a region known to be dominated by *T. aduncus*, while one dolphin apparently feeding offshore was from a region (off Muscat) dominated by *T. truncatus*. Furthermore, those dolphins feeding inshore showed a diet that includes species such as the croaker, *Otolithes ruber*, that occur on sandy and muddy substrates (Ponnampalam *et al*. 2012).

Morphological differences (within *T. aduncus*)

Differences between the *T. aduncus* lineages were less than among species for most linear measures. However, several measures of cranial/rostral width, as well as orbit length, were identified as important characters for discriminating between *T. aduncus* lineages, with the *T. aduncus* holotype being larger and wider in all characters analysed than the Arabian Sea conspecifics (Figure 4). Discriminatory analyses using geometric morphometric data suggest a degree of significant differentiation in cranial geometry between *T. aduncus* lineages, particularly in lateral view. Lateral shape was also independent of allometric effects. Visualisations of the shape differences suggest a more slender or elongated skull in the Arabian Sea lineage than the holotype lineage, with shape differences in the temporal fossae, orbits or both.

More slender/elongated skulls in AS-Ta might be expected if the lineage were adapted to foraging in an environment with high turbidity, for example, as seen in river dolphins (Cassens *et al*. 2000; Smith & Reeves, 2012). This may give individuals greater 'reach' in pursuit of highly mobile prey. Head shape has also been proposed to be related to adaptation for efficient echolocation (eg. Frainer *et al*. 2021). Changes to the orbit of the AS-Ta lineage might also be a result of living in a more turbid environment, again, the extreme being found in river dolphins, which have small eyes (Herald *et al*. 1969). Indeed, off Pakistan and India, river influx (e.g. the Indus river delta) discharges freshwater and organic material, resulting in a brackish and turbid coastal environment (Longhurst, 2006). If this was true, we might expect to see similar morphological characteristics in other coastal dolphin species in the region. Common dolphins (Jefferson & Van Waerebeek, 2002), spinner dolphins (Van Waerebeek *et al*. 1999) and humpback dolphins (Jefferson & Van Waerebeek, 2004) in the same general study region, all appear to be converging on a similar 'long-beaked' morphotype, suggesting different dolphin species are adapting to local environmental conditions in similar ways.

Given the overlap in range between these two *T. aduncus* lineages, it is conceivable that hybridization and introgression are responsible for the overlap in cranial morphology. For example, two specimens from Oman (ONHM 1975 and 3079), identified as AS-Ta from mtDNA control region sequences, consistently clustered with the Hol-Ta specimens in both LDA (Figure 6) and RF (Figure 7) analyses conducted on linear measurements. However, these specimens were geometrically close to Hol-Ta specimens in CVA analyses, conducted on geometric morphometric data (Figure 9). One possible explanation would be allometry picked up in the linear measurements, however, sample sizes for these groups were small. Future morphological analyses would benefit from further specimens from the region, and

further afield, including specimens from the Australasian *T. aduncus* lineage (Wang *et al.* 2000).

Morphological distinction between the *T. aduncus* lineages is suggestive of adaptation to local habitats in the northwest Indian Ocean and provides support for a separate conservation unit in the region (see Reeves *et al*. 2004), although analyses with further representation for the AS-Ta lineage is recommended. The extent of divergence between *T. truncatus* and *T. aduncus* compared to differences between the AS-Ta and Hol-Ta forms is consistent with the proposition in Moura *et al*. (2020) that the latter may reflect subspecific differences rather than at the species level. Morphological differentiation reported herein will be of broad interest to the study of evolutionary processes in highly mobile marine taxa, particularly as these *T. aduncus* lineages are either experiencing secondary contact (after divergence in allopatry) or are diverging in sympatry.

Conclusion

The morphological differences we found between lineages likely reflect differences in the ecology of these populations that will require further investigation through dietary and life-history studies. The outcomes of such analyses will be of interest to conservation initiatives in the region. Moreover, there is increasing evidence to suggest that this region is home to a number of unique/isolated cetacean evolutionary significant units (ESU, e.g. for a regional population of blue whales; Cerchio *et al*. 2020), and is therefore important for the study of evolutionary processes in cetaceans. It is imperative, particularly in light of the alarming increase in threats to coastal species (such as *T. aduncus*) from human development and fisheries practices in the region, that these ESUs are given the required recognition and protection so that their conservation can be managed effectively and without delay.

Acknowledgements

This study was partly supported by the Environment Society of Oman (ESO) and Five Oceans Environmental Services LLC. Oman specimens were curated at the Oman Natural History Museum (ONHM) and collected by The Oman Whale and Dolphin Research Group, Michael Gallagher and various independent scientists and volunteers that have worked in Oman. Thanks are due to Hanan Al Nabhani for her assistance at the ONHM, and we are very grateful to Mr. Mohammed for all of his careful work retrieving specimens and kind assistance with sampling. Specimens from Pakistan and Iran were collected by Pilleri and Gihr on various expeditions in the region and were curated at the Museum am Löwentor,

Staatliches Museum für Naturkunde, in Stuttgart, Germany (SMNS). Thank you to Dr. Doris Mörike from the SMNS for her time retrieving skulls and assisting with photographing, measuring and sampling them. Further thanks are due to Oman's Environment Authority (former Ministry of Environment and Climate Affairs) for providing permits to collect specimens on various historic expeditions and for shipping samples. We are grateful to Eric Archer and an anonymous reviewer for their constructive comments.

References

Adams DC, Otárola-Castillo E. 2013. Geomorph: An R package for the collection and analysis of geometric morphometric shape data. *Methods in Ecology and Evolution*. 4(4): 393-399.

Amaha A. 1994. Geographic variation of the common dolphin, *Delphinus delphis* (Odontoceti: Delphinidae). Ph.D. thesis, Graduate School of Fisheries Tokyo University of Fisheries, Tokyo.

Anderson RC. 2014. Cetaceans and tuna fisheries in the Western and Central Indian Ocean. *International Pole and Line Federation Technical Report* 2.

Baldwin RM, Collins M, Van Waerebeek K, Minton G. 2004. The Indo-Pacific humpback dolphin of the Arabian region: A status review. *Aquatic Mammals*. 30(1): 111-124.

Brown CM, Arbour JH, Jackson DA. 2012. Testing of the effect of missing data estimation and distribution in morphometric multivariate data analyses. *Systematic Biology*. 61(6): 941-54.

Cassens I, Vicario S, Waddell VG, Balchowsky H, Van Belle D, Ding W, Fan C, Lal Mohan R, Simões-Lopes PC, Bastida R, Meyer A, Stanhope MJ, Milinkovitch MC. 2000. Independent adaptation to riverine habitats allowed survival of ancient cetacean lineages. *Proceedings of the National Academy of Sciences*. 97(21): 11343-11347.

Charlton-Robb K, Gershwin LA, Thompson R, Austin J, Owen K, Mckechnie S. 2011. A new dolphin species, the Burrunan dolphin *Tursiops australis* sp. *nov.*, endemic to southern Australian coastal waters. *Plos One*. **6(9):** e24047.

Collins T, Minton G, Baldwin R, Van Waerebeek K, Hywel-Davies A, Cockcroft V. 2002. A preliminary assessment of the frequency, distribution and causes of mortality of beach cast cetaceans in the Sultanate of Oman, January 1999 to February 2002. *IWC Scientific Committee Document.* SC/54/O4. pp.13.

Dalebout ML, Mead JG, Baker CS, Baker AN, Helden AL. 2002. A new species of beaked whale *Mesoplodon perrini* sp. n. (Cetacea: Ziphiidae) discovered through phylogenetic analyses of mitochondrial DNA sequences. *Marine Mammal Science*. 18(3): 577-608.

Dornburg A, Friedman M, Near TJ. 2015. Phylogenetic analysis of molecular and morphological data highlights uncertainty in the relationships of fossil and living species of

Elopomorpha (Actinopterygii: Teleostei). *Molecular Phylogenetics and Evolution*. 89: 205-18.

Dunn O J. 1964. Multiple comparisons using rank sums. *Technometrics*, 6: 241-252.

Frainer G, Huggenberger S, Moreno IB, Plön S, Galatius A. (2021). Head adaptation for sound production and feeding strategy in dolphins (Odontoceti: Delphinida). *Journal of Anatomy*, *238*(5): 1070-1081.

Gray HWI, Nishida S, Welch AJ, Moura AE, Tanabe S, Kiani MS, Culloch R, Möller L, Natoli A, Ponnampalam LS, Minton G, Gore M, Collins T, Willson A, Baldwin R, Holezel R. 2018. Cryptic lineage differentiation among Indo-Pacific bottlenose dolphins (*Tursiops aduncus*) in the northwest Indian Ocean. *Molecular Phylogenetics and Evolution*. 122: 1-4.

Gray HWI, Chen I, Moura AE, Natoli A, Nishida S, Tanabe S, Minton G, Ponnampalam LS, Kiani MS, Culloch R, Gore M, Särnblad A, Omar A, Berggren P, Collins T, Willson A, Baldwin R, Hoelzel R. 2021. Comparative biogeography and the evolution of population structure for bottlenose and common dolphins in the Indian Ocean. *Journal of Biogeography*. 48: 1654-1668.

He F, Mazumdar S, Tang G, Bhatia T, Anderson SJ, Dew MA, Krafty R, Nimgaonkar V, Deshpande S, Hall M, Reynolds CF. (2017). Non-parametric MANOVA approaches for non-normal multivariate outcomes with missing values. *Communications in Statistics - Theory and Methods*. 46(14): 7188–7200.

Herald ES, Brownell RL, Frye FL, Morris EJ, Evans WE, Scott AB. 1969. Blind river dolphin: First side-swimming cetacean. *Science*. 166(3911): 1408- 1410.

Hersh SL, Odell DK, Asper ED. 1990. Sexual dimorphism in bottlenose dolphins from the east coast of Florida. *Marine Mammal Science*. 6(4): 305-315.

Hershkovitz P. 1966. Catalog of living whales. Smithsonian Institution Bulletin 246. pp.256

IWC 1999. Annex I Report of the Standing Sub-Committee on Small Cetaceans. *Journal of Cetacean Research and Management* (Suppl.): 211-225.

Jayasankar P, Anoop B, Reynold P, Krishnakumar PK, Kumaran PL, Afsal VV, Anoop AK. 2008. Molecular identification of delphinids and finless porpoise (Cetacea) from the Arabian Sea and Bay of Bengal. *Zootaxa*. 1853: 57-67.

Jefferson TA, Van Waerebeek K. 2002. The taxonomic status of the nominal dolphin species *Delphinus tropicalis* van Bree, 1971. *Marine Mammal Science*. 18(4): 787-818.

Jefferson TA, Van Waerebeek K. 2004. Geographic variation in skull morphology of humpback dolphins (*Sousa* spp.). *Aquatic Mammals*. 30: 3-17.

Kaufman L, Rousseeuw PJ. 2009. Finding groups in data: An introduction to cluster analysis. John Wiley & Sons.

Kemper CM. 2004. Osteological variation and taxonomic affinities of bottlenose dolphins, *Tursiops* spp., from South Australia. *Australian Journal of Zoology*. 52(1): 29-48.

Kim JO, Curry J. 1977. The treatment of missing data in multivariate analysis. *Sociological Methods and Research*. 6(2). 215-240.

Klingenberg CP, Monteiro LR. 2005. Distances and directions in multidimensional shape spaces: Implications for morphometric applications. *Systematic Biology*. 54(4): 678-688.

Klingenberg CP. 2011. MorphoJ: An integrated software package for geometric morphometrics. *Molecular Ecology Resources*. 11(2): 353-357.

Liaw A, Wiener M. (2002). Classification and regression by randomForest. *R News.* 2(3): 18-22.

Longhurst A. 2006. *Ecological geography of the sea*. Academic Press, Amsterdam, Boston, MA.

Mace GM. 2004. The role of taxonomy in species conservation. *Philosophical Transactions of the Royal Society of London. Series B, Biological Sciences*. 359(1444): 711-719.

Maechler M, Rousseeuw P, Struyf A, Hubert M, Hornik K, Studer M, Roudier P. 2015. Cluster: Cluster analysis basics and extensions. R Package Version 2.0.3.

Mead JG, Fordyce RE. 2009. *The therian skull: A lexicon with emphasis on the odontocetes*. Smithsonian Contributions to Zoology. pp. 248.

Minton G, Collins TJQ, Findlay KP, and Baldwin, R. 2010. Cetacean distribution in the coastal waters of the Sultanate of Oman. *Journal of Cetacean Research and Management*. 11(3): 301-313.

Mitteroecker P, Gunz P. 2009. Advances in geometric morphometrics. *Evolutionary Biology*. 36(2): 235-247

Moura AE, Nielsen SCA, Vilstrup JT, Moreno-Mayar JV, Gilbert MTP, Gray HWI, Natoli A, Möller L, Hoelzel AR. (2013). Recent diversification of a marine genus (*Tursiops* spp.) tracks habitat preference and environmental change. *Systematic Biology*. 62(6): 865-877.

Moura AE, Shreves K, Pilot M, Andrews KR, Moore DM, Kishida T, Möller L, Natoli A, Gaspari S, McGowen M, Chen, I, Gray H, Gore, M, Culloch R, Kiani M, Sarrouf-Wilson M, Bulushi A, Collins T, Baldwin R, Willson A, Minton G, Ponnampalam L, Hoelzel AR. (2020). Phylogenomics of the genus *Tursiops* and closely related Delphininae reveals extensive reticulation among lineages and provides inference about eco-evolutionary drivers. *Molecular Phylogenetics and Evolution*. 146: 106756.

Natoli A, Peddemors VM, Rus Hoelzel A. (2004). Population structure and speciation in the genus *Tursiops* based on microsatellite and mitochondrial DNA analyses. *Journal of Evolutionary Biology*. 17(2): 363-375.

Pedersen TL, Hughes S, Qiu X. (2016). *densityclust*: Clustering by fast search and find of density peaks. *R package version 0.2*.

Perrin WF, Robertson KM, van Bree PJH, Mead JG. (2007). Cranial description and genetic identity of the holotype specimen of *Tursiops aduncus* (Ehrenberg, 1832). *Marine Mammal Science*. 23(2): 343-357.

Perrin WF, Thieleking JL, Walker WA, Archer FI, Robertson KM. (2011). Common bottlenose dolphins (*Tursiops truncatus*) in California Waters: Cranial differentiation of coastal and offshore ecotypes. *Marine Mammal Science*. 27(4): 769-792.

Pilleri G, Gihr M. (1972). Contribution to the knowledge of the cetaceans of Pakistan with particular reference to the genera *Neomeris*, *Sousa*, *Delphinus* and *Tursiops* and description of a new Chinese porpoise (*Neomeris asiaeorientalis*). *Investigations on Cetacea*. 4: 107-162.

Ponnampalam LS, Collins TJQ, Minton G, Schulz I, Gray H, Ormond RFG, Baldwin RM. (2012). Stomach contents of small cetaceans stranded along the Sea of Oman and Arabian Sea coasts of the Sultanate of Oman. *Journal of the Marine Biological Association of the United Kingdom*. 92(8): 1699-1710.

R Core Team (2013). *R: A Language and Environment for Statistical Computing*. R Foundation for Statistical Computing, Vienna, Austria. http://www.R-project.org

Reeves R, Perrin W, Taylor B, Baker C, Mesnick S. (2004). Report of the workshop on shortcomings of cetacean taxonomy in relation to needs of conservation and management, April 30-May 2, 2004, La Jolla, California. US Department of Commerce, National Oceanic and Atmospheric Administration, National Marine Fisheries Service, Southwest Fisheries Science Center.

Rodriguez A, Laio A. (2014). Clustering by fast search and find of density peaks. *Science*. 344(6191): 1492-1496.

Rohlf F. (2005). TPSDIG, Version 2.04. Department of Ecology and Evolution, State University of New York, Stony Brook, New York.

Ross GJB, Cockcroft VG. (1990). Comments on Australian bottlenose dolphins and taxonomic stock of *Tursiops aduncus* (Ehrenberg 1832). In: Leatherwood S, Reeves RR, eds. *The Bottlenose Dolphin*. Academic Press Limited 24-48 Oval Road, London NW1 7DX, 101-128.

Ross GJ. 1977. The taxonomy of bottlenosed dolphins *Tursiops* species in South African waters, with notes on their biology. *Annals of the Cape Provincial Museums, Natural History*. 11: 259-327.

Shirakihara M, Yoshida H, Shirakihara K. (2003). Indo-Pacific bottlenose dolphins *Tursiops aduncus* in Amakusa, western Kyushu, Japan. *Fisheries Science*. 69(3): 654-656.

Singleton M. 2002. Patterns of cranial shape variation in the Papionini (Primates: Cercopithecinae). *Journal of Human Evolution*. 42(5): 547-578.

Slice D. 1998. MORPHEUS et al.: Software for morphometric research. Department of Ecology and Evolution, State University of New York, Stony Brook, New York.

Smith BD, Reeves RR. 2012. River cetaceans and habitat change: Generalist resilience or specialist vulnerability? *Journal of Marine Biology*. 2012: 1-11.

Van Bocxlaer B, Schultheiß R. (2010). Comparison of morphometric techniques for shapes with few homologous landmarks based on machine-learning approaches to biological discrimination. *Paleobiology*. 36(3): 497-515.

Van Waerebeek K, Gallagher M, Baldwin R, Papastavrou V, Mustafa AL. 1999. Morphology and distribution of the spinner dolphin, *Stenella longirostris*, rough toothed dolphin, *Steno bredanensis* and melon-headed whale, *Peponocephala electra* from waters off the Sultanate of Oman. *Journal of Cetacean Research and Management*. 1(2): 167-177.

Venables W, Ripley B. 2002. *'Modern Applied Statistics with S-PLUS', Statistics and Computing*. Springer Science & Business Media. pp.498

Wang L, Sarnthein M, Erlenkeuser H, Grimalt J, Grootes P, Heilig S, Ivanova E, Kienast M, Pelejero C, Pflaumann U. 1999. East Asian monsoon climate during the late Pleistocene: High-resolution sediment records from the South China Sea. *Marine Geology*. 156(1): 245-284.

Wang JY, Chou L-S, White BN. 2000. Osteological differences between two sympatric forms of bottlenose dolphins (genus *Tursiops*) in Chinese Waters. *Journal of Zoology*. 252(2): 147-162.

Weihs C, Ligges U, Luebke K, Raabe N. 2005. *klaR* analyzing German business cycles. In: Baier D, Decker R and Schmidt-Thieme L, eds. *Data Analysis and Decision Support*. Springer-Verlag, Berlin. pp.335-343.

Yang Z, Rannala B. 2012. Molecular phylogenetics: principles and practice. *Nature Reviews Genetics.* 13: 303-314.

Data Availability Statement

Geometric morphometric data and linear measurement data utilised in analyses herein are available on Dryad at XXX

Supporting Information

Further information is available in the supplementary documentation.

Table 1. Coefficients of linear discriminants for most important morphometric characters identified in a stepwise MANOVA. LD = linear discriminant. Refer to Figure 2 and Table S1 for character descriptions.

Character	LD1	LD2
RW60	0.208	0.031
GPOW	-0.023	-0.217
ZW	-0.038	0.221
LAL	0.179	0.023
RWM	0.099	-0.064

Table 2. Leave-one-out cross-validation scores given using linear discriminant and, in parentheses, the random forest model. Hol-Ta = *Tursiops aduncus* holotype lineage; AS-Ta = *T. aduncus* Arabian Sea lineage; Tt = *T. truncatus*; OOB = 'out of box'.

True Group	Classified as AS-Ta	Classified as Hol-Ta	Classified as Tt	*n*	Misclassification Rate (%)	Total *n*	Overall Misclassification Rate / OOB estimate error rate for random forest (%)
AS-Ta	4 (5)	5 (4)	0 (0)	9	56 (44)	46	24 (13.04)
Hol-Ta	5 (2)	24 (27)	0 (0)	29	17 (7)		
Tt	1 (0)	0 (0)	7 (8)	8	13 (0)		

Table 3. Canonical Variates Analysis pairwise Mahalanobis and Procrustes distances between groups given for dorsal, ventral and lateral aspect geomorphometric data. Associated P-values generated from permutation tests (1000 permutations). Hol-Ta = *Tursiops aduncus* holotype lineage; AS-Ta = *T. aduncus* Arabian Sea lineage; Tt = *T. truncatus*.

	Dorsal				Ventral				Lateral			
	Mahalanobis		Procrustes		Mahalanobis		Procrustes		Mahalanobis		Procrustes	
Groups	**Distance**	***P***	**Distance**	***P***	**Distance**	***P***	**Distance**	***P***	**Distance**	***P***	**Distance**	***P***
Hol-Ta - AS-Ta	1.7978	0.0425	0.0162	0.2087	2.4461	0.0002	0.0160	0.0900	3.1164	<0.0001	0.0283	0.0012
Hol-Ta - Tt	3.8218	<0.0001	0.0381	0.0001	6.2860	<0.0001	0.0423	<0.0001	5.5021	<0.0001	0.0443	<0.0001
AS-Ta - Tt	4.4346	<0.0001	0.0451	0.0003	6.7245	<0.0001	0.0474	<0.0001	6.4914	<0.0001	0.0552	0.0001

Table 4. Discriminant Function Analysis pairwise Mahalanobis and Procrustes distances between groups given for dorsal, ventral and lateral aspect geomorphometric data. Associated P-values generated from permutation tests (1000 permutations). Hol-Ta = *Tursiops aduncus* holotype lineage; AS-Ta = *T. aduncus* Arabian Sea lineage; Tt = *T. truncatus*.

	Dorsal				**Ventral**				**Lateral**			
	Mahalanobis		**Procrustes**		**Mahalanobis**		**Procrustes**		**Mahalanobis**		**Procrustes**	
Groups	**Distance**	***P***	**Distance**	***P***	**Distance**	***P***	**Distance**	***P***	**Distance**	***P***	**Distance**	***P***
Hol-Ta - AS-Ta	1.6897	0.6390	0.016203	0.2050	2.6591	0.3480	0.015959	0.0740	4.1761	0.0340	0.028314	0.0020
Hol-Ta - Tt	4.0965	<0.0001	0.038059	<0.0001	8.4090	<0.0001	0.042264	<0.0001	5.9092	0.0010	0.044307	<0.0001
AS-Ta - Tt	19.1588	0.0780	0.045052	<0.0001	6.7666	0.0070	0.047444	<0.0001	11.1106	<0.0001	0.055188	<0.0001

Table 5. DFA pairwise group allocation table and cross-validation scores for dorsal, ventral and lateral aspect geometric morphometric data. Hol-Ta = *Tursiops aduncus* holotype lineage; AS-Ta = *T. aduncus* Arabian Sea lineage; Tt = *T. truncatus*.

		Dorsal				**Ventral**				**Lateral**			
		Group Assigned				**Group Assigned**				**Group Assigned**			
Hol-Ta – AS-Ta	**True Group**	**Hol-Ta**	**AS-Ta**	**Total**	**% Correct**	**Hol-Ta**	**AS-Ta**	**Total**	**% Correct**	**Hol-Ta**	**AS-Ta**	**Total**	**% Correct**
Discriminant Function	Hol-Ta	25	7	32	78	30	3	33	91	32	1	33	97
	AS-Ta	1	9	10	90	1	9	10	90	0	10	10	100
Cross-Validation	Hol-Ta	21	11	32	66	20	13	33	61	27	6	33	82
	AS-Ta	6	4	10	40	6	4	10	40	3	7	10	70
		Group Assigned				**Group Assigned**				**Group Assigned**			
Hol-Ta – Tt	**True Group**	**Hol-Ta**	**Tt**	**Total**	**% Correct**	**Hol-Ta**	**Tt**	**Total**	**% Correct**	**Hol-Ta**	**Tt**	**Total**	**% Correct**
Discriminant Function	Hol-Ta	32	0	32	100	33	0	33	100	33	0	33	100
	Tt	0	9	9	100	0	9	9	100	0	9	9	100
Cross-Validation	Hol-Ta	29	3	32	91	32	1	33	97	29	4	33	88
	Tt	2	7	9	78	2	7	9	78	2	7	9	78
		Group Assigned				**Group Assigned**				**Group Assigned**			
AS-Ta – Tt	**True Group**	**AS-Ta**	**Tt**	**Total**	**% Correct**	**AS-Ta**	**Tt**	**Total**	**% Correct**	**AS-Ta**	**Tt**	**Total**	**% Correct**
Discriminant Function	AS-Ta	10	0	10	100	10	0	10	100	10	0	10	100
	Tt	0	9	9	100	0	9	9	100	0	9	9	100
Cross-Validation	AS-Ta	7	3	10	70	7	3	10	70	9	1	10	90
	Tt	3	6	9	67	3	6	9	67	4	5	9	56

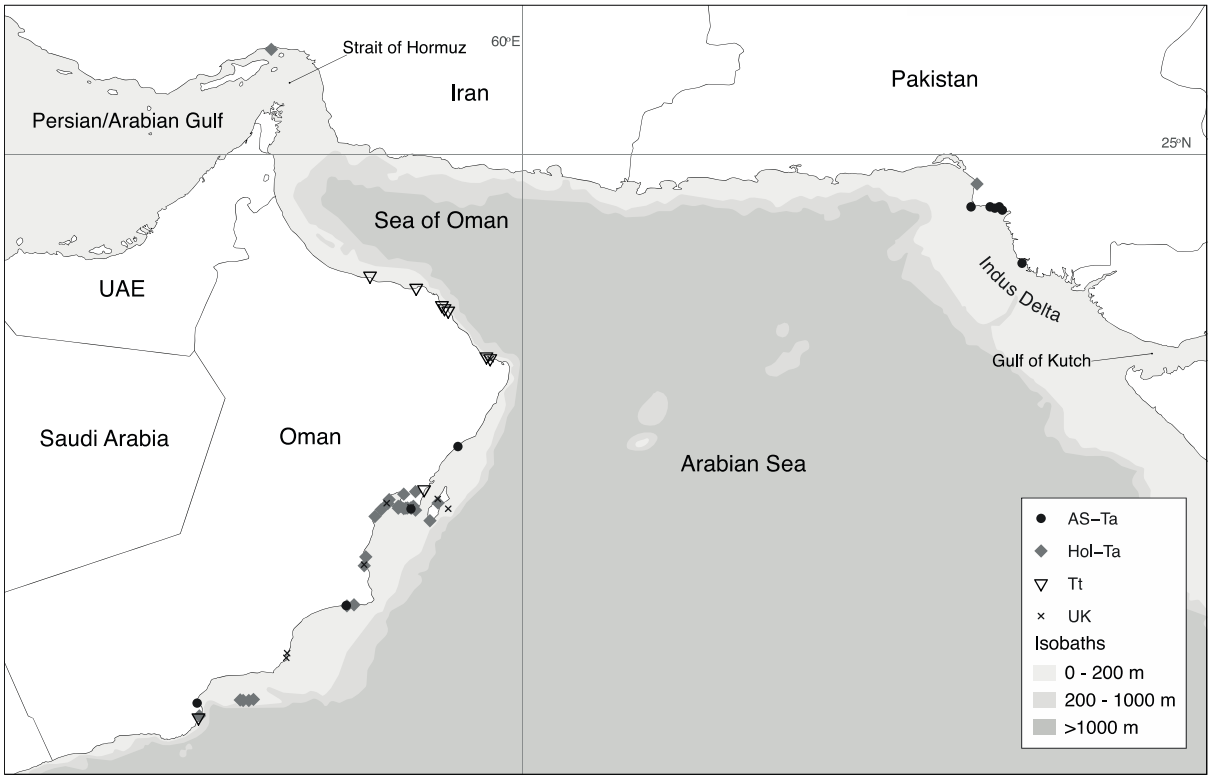

Figure 1. Map showing locations of specimens utilised in various analyses. Specimens were omitted from analyses where they did not meet certain criteria e.g. were cranially immature or too damaged (see Methods and Results). AS-Ta = *Tursiops aduncus* Arabian Sea lineage; Hol-Ta = *T. aduncus* holotype lineage; Tt = *T. truncatus*; Unknown = specimens unassigned to a genetic lineage (where DNA could not be extracted).

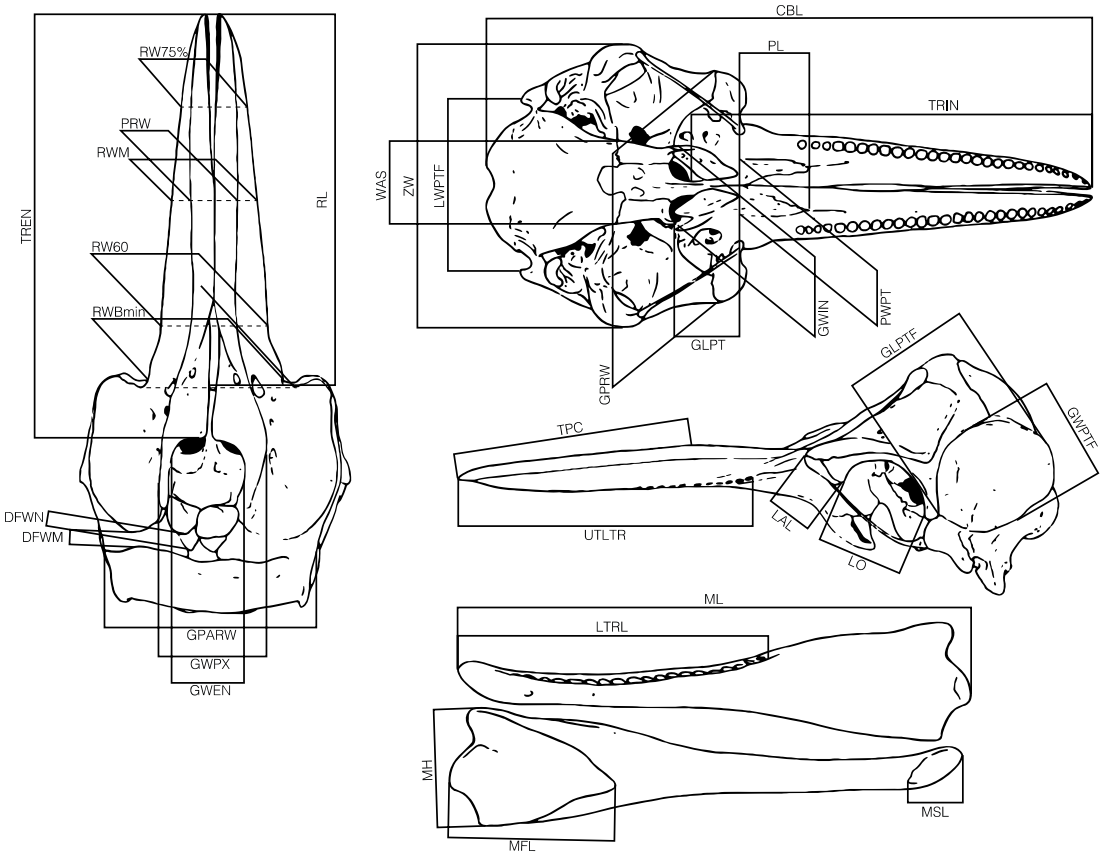

Figure 2. Morphological measurements taken, as adapted from Perrin (1975). BL, BW, POL, TTL, TTU, and TWTMJ not illustrated. See Table S1 for character descriptions and associated references.

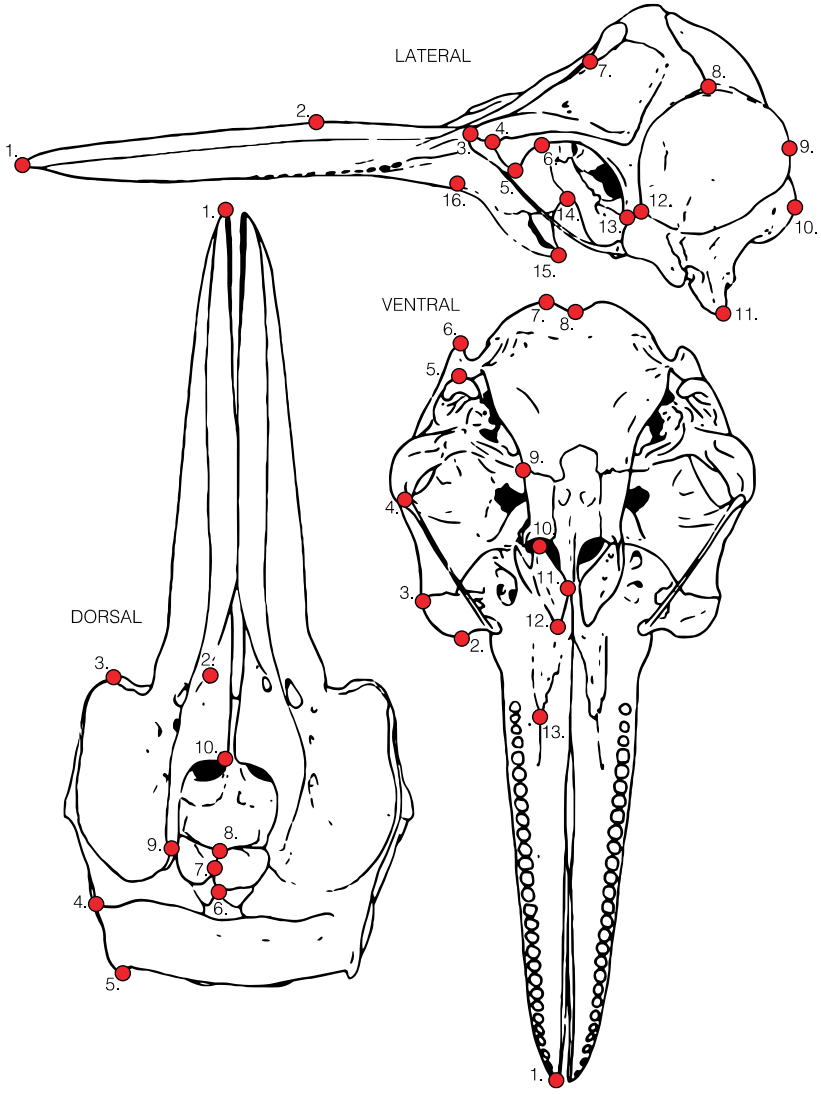

Figure 3. Positioning of landmarks used in geometric morphometric analysis. See Table S2 for descriptions and associated references.

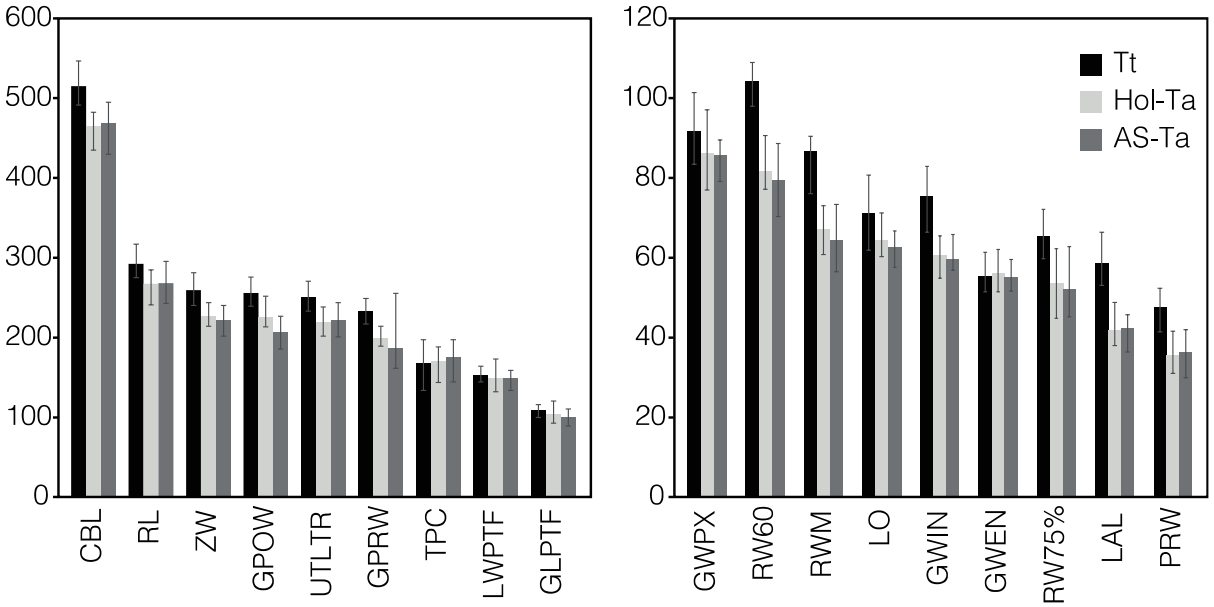

Figure 4. Summary of mean measurements taken (mm) of 18 morphological characters used in analyses for specimens assigned to a genetic lineage based on mtDNA (see Fig S1). AS-Ta = *Tursiops aduncus* Arabian Sea lineage; Hol-Ta = *T. aduncus* holotype lineage; Tt = *T. truncatus*. Bars indicate range of measurements for each character. For sample sizes, refer to measurement tables. For character descriptions, refer to Table S1.

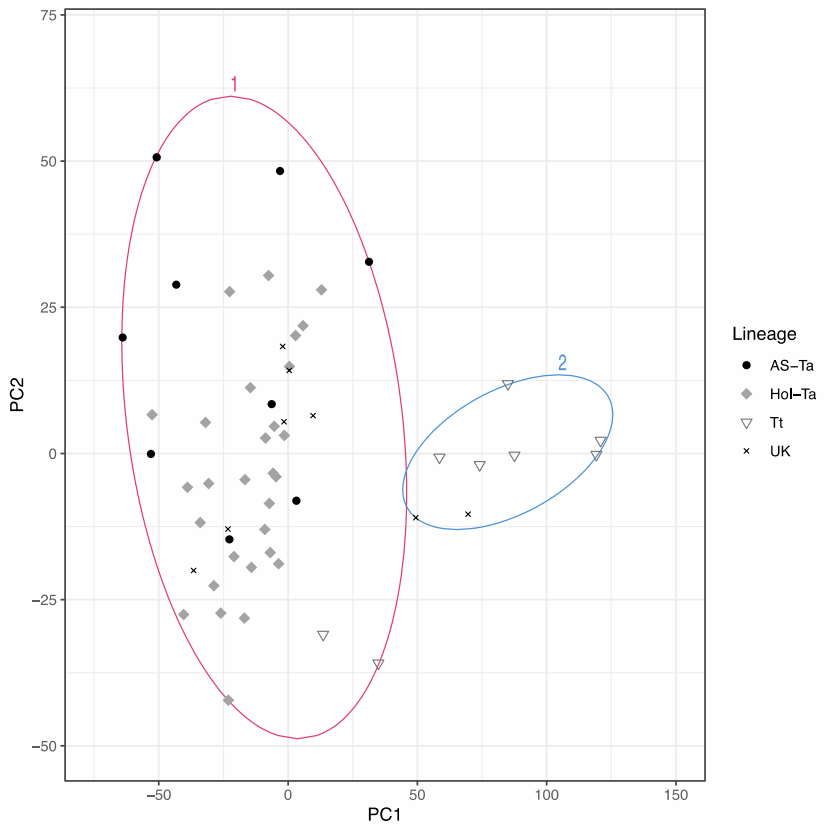

Figure 5. PCA of linear measurements; PC (principal component) 1 against PC2. Specimens were assigned to clusters based on the *k*-medoids algorithm and drawn using the *clusplot* function in the *cluster* R package (Maechler *et al*. 2015). AS-Ta = *Tursiops aduncus* Arabian Sea lineage; Hol-Ta = *T. aduncus* holotype lineage; Tt = *T. truncatus*; UK = specimens unassigned to a genetic lineage (unknown).

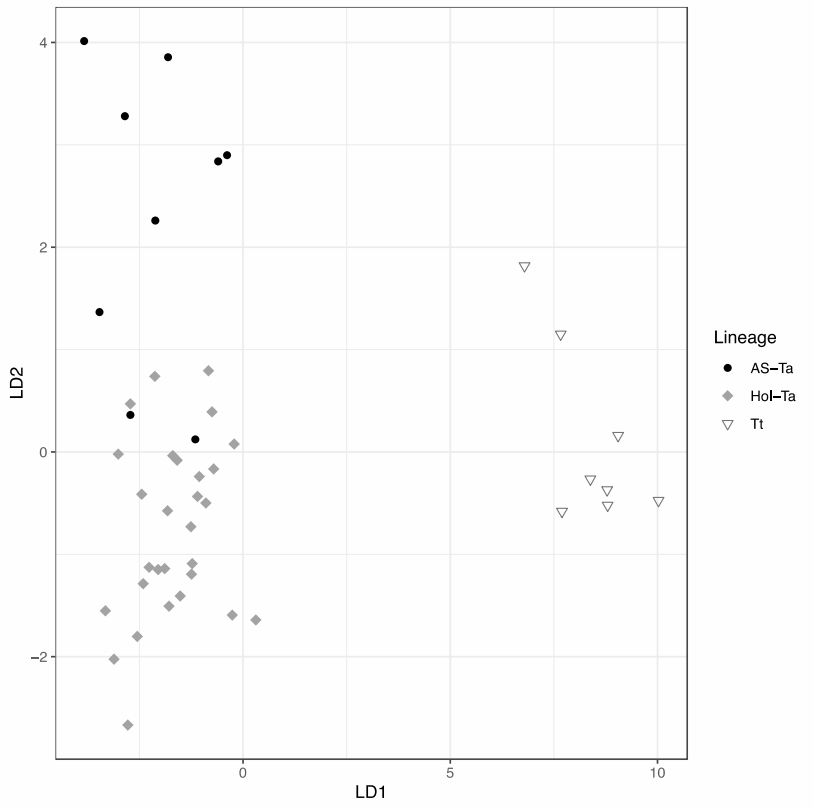

Figure 6. Linear Discriminant Analysis of morphometric measurements. LD = linear discriminant; Hol-Ta = *Tursiops aduncus* holotype lineage; AS-Ta = *T. aduncus* Arabian Sea lineage; Tt = *T. truncatus*.

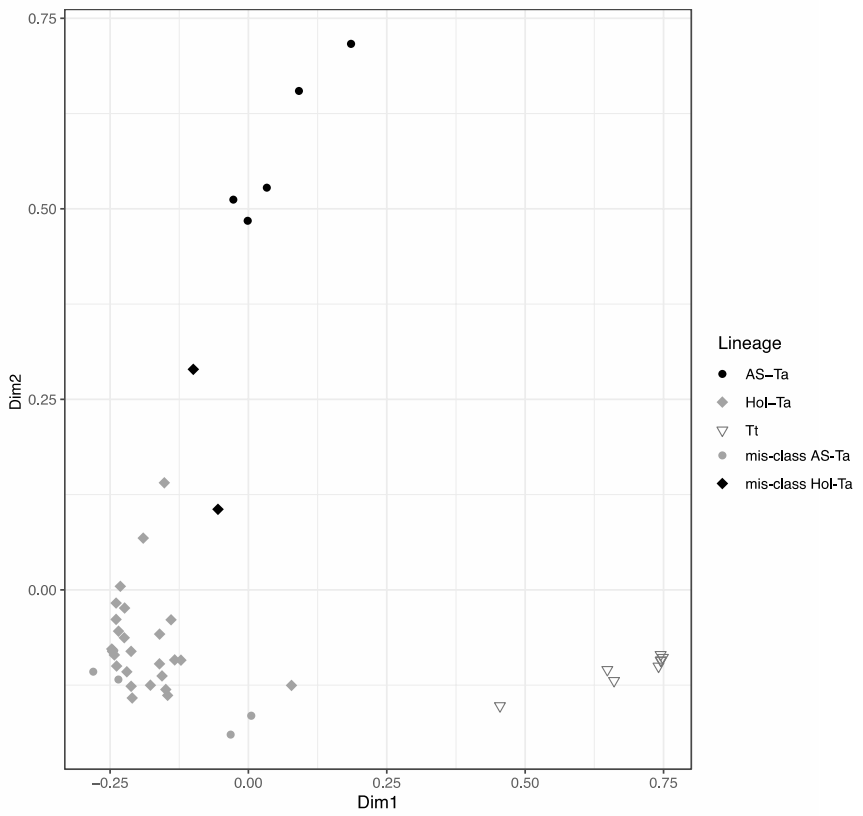

Figure 7. MDS plot of proximity measures for each specimen assigned in a random forest model generated in R using the *randomForest* package. Dim1 = Dimension 1; Dim2 = Dimension 2; Hol-Ta = *Tursiops aduncus* holotype lineage; AS-Ta = *T. aduncus* Arabian Sea lineage; Tt = *T. truncatus*; mis-class AS-Ta = Arabian Sea lineage specimens (assigned genetically) mis-identified by the model as Hol-Ta; mis-class Hol-Ta = Holotype lineage specimens (assigned genetically) mis-identified by the model as AS-Ta.

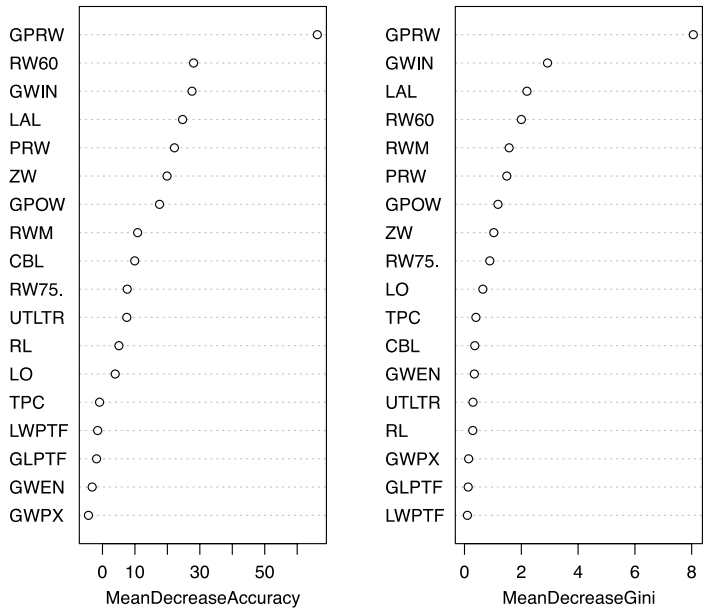

Figure 8. Measures of importance (mean decrease accuracy and Gini) of the different characters to the random forest model as generated in R using the *randomForest* package. See Figure 2 and Table S1 for character descriptions.

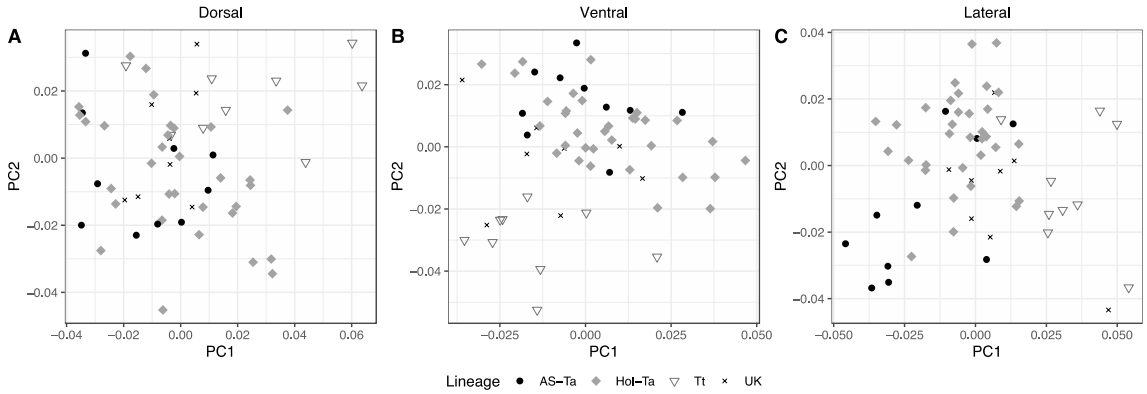

Figure 9. PCA in A) dorsal B) ventral and C) lateral aspect based on geomorphometric data. For each plot, PC1 = x-axis; PC2 = y-axis; AS-Ta = *Tursiops aduncus* Arabian Sea lineage; Hol-Ta = *T. aduncus* holotype lineage; Tt = *T. truncatus*; UK = specimens unassigned to a genetic lineage (unknown).

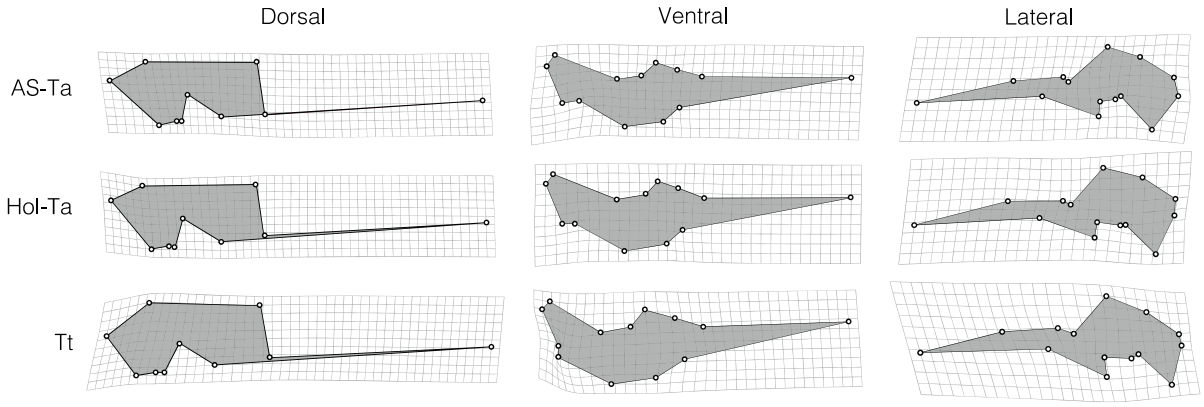

Figure 10. Visual comparisons of average group shapes, AS-Ta, Hol-Ta and Tt, for all aspects. Thin-plate spline transformation grids, showing warping from the total average configuration, with overlaid wireframe graphs are illustrated. Hol-Ta = *Tursiops aduncus* holotype lineage; AS-Ta = *T. aduncus* Arabian Sea lineage; Tt = *T. truncatus*.

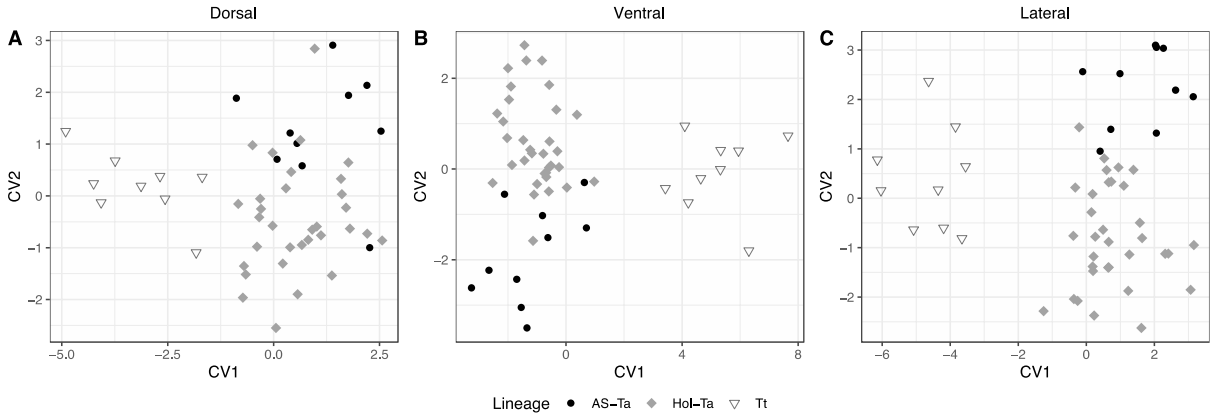

Figure 11. Canonical Variates Analysis for geomorphometric data in A) dorsal, B) ventral and C) lateral aspect. x-axis = canonical variate (CV) 1; y-axis = CV2; AS-Ta = *Tursiops aduncus* Arabian Sea lineage; Hol-Ta = *T. aduncus* holotype lineage; Tt = *T. truncatus*.